Boiling in variable gravity under the action of an electric field: results of parabolic flight experiments

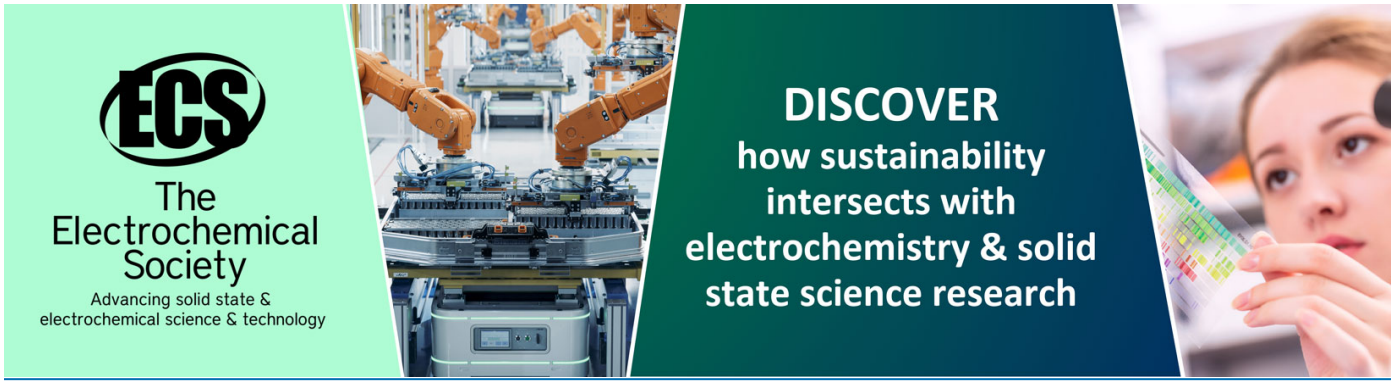

Journal of Physics: Conference Series **327** (2011) 012039 doi:10.1088/1742-6596/327/1/012039

Boiling in variable gravity under the action of an electric field: results of parabolic flight experiments

P Di Marco [1], R Raj [2], J Kim [2]

[1]Department of Energy and Systems Engineering, University of Pisa, Largo Lazzarino 1, 56122 Pisa, Italy

[2]Department of Mechanical Engineering, University of Maryland,College Park, MD 20742, USA

E-mail: p.dimarco@ing.unipi.it

Abstract. Results from the variable gravity pool boiling experiments performed during the 52nd ESA parabolic flight campaign are reported in this paper. During a typical parabola, the gravity acceleration changes from $1.8g_E$ (high gravity) to ~$0g_E$ (low gravity) and finally back to $1.8g_E$. The two high gravity periods and the microgravity period are each roughly maintained for 20 seconds while the transition from high gravity to low gravity and vice versa occurs over a period of 3–5 seconds. Use of the high feedback frequency microheater array allowed quasi-steady boiling data over the continuous range of gravity levels ($0g_E$-$1.8g_E$). The experimental apparatus consisted of a boiling chamber with a 7x7 mm^2 microheater array in a 10x10 configuration. Each heater in the array was individually controlled to maintain a constant temperature. The array could be operated in a full configuration or a selectively powered reduced set of 3x3 heaters. Experiments were performed with FC-72 as the test fluid, the pressure was maintained at a constant value between 1 and 1.13 atm and the subcooling ranged from 27 to 11 K. An external electric field was imposed over the boiling surface by means of a grid consisting of 4 rods, laid parallel to the surface; voltages up to 10 kV were applied. The electric field was effective in reducing the size of the detaching bubbles, and increasing the heat transfer compared to the values in low-g, although its effectiveness decayed as the heat flux/superheat increased. The current results compared well with previous results obtained in the ARIEL apparatus that was operated in orbital flight.

1. Introduction

Investigating and assessing boiling performance in reduced gravity conditions is of paramount importance for the design of efficient heat exchange devices for future space and planetary missions. The problem has been addressed since the early 60s [1] and recently reviewed by Di Marco, Kim and Ohta [2] and Di Marco [3]. In particular, significant contributions were made by Straub and coworkers [4] and Merte [5] who performed numerous experiments on different platforms. It has been shown that – as could be easily expected –bubble detachment, and mostly vapor removal away from the surface are impaired by the reduction of buoyancy forces; however different forces, including inertia, surface tension and Marangoni convection come into play and partially replace the absent buoyancy force.

Recently, Kim and coworkers [6] took advantage of the injection phase of parabolic flight to operate a heater in quasi-steady condition in variable gravity. As the gravity level changed, a sharp transition in the heat transfer mechanism was observed at a threshold gravity level. Below this

threshold (low-g regime), a nondeparting coalesced bubble governed the heat transfer and the effect of residual gravity was small. Above this threshold (high-g regime), bubble growth and departure dominated the heat transfer and gravity effects became more important. Heat flux was found to be heater size dependent only in the low-g regime. Significantly, the slope of the heat flux versus acceleration curve was different in the two regimes, ruling out the possibility of a unified power law dependence across all gravity levels.

Di Marco and Grassi [7,8] widely explored the possibility to apply an electric field to the boiling systems in order to have the buoyancy forces replaced by the electrostatic one. Several experiments on different platforms demonstrated that the boiling heat transfer could be improved in this way. In some cases, the boiling performance with electric field in low-g was similar to what could be obtained in normal boiling in terrestrial gravity.

This paper describes the results obtained in a pool boiling experiment carried out during the ESA 52ndparabolic flight campaign in May, 2010. The experiment apparatus consisted of a boiling chamber filled with FC-72, with a 7x7 mm^2 microheater array in a 10x10 configuration (four corners missing, 96 heaters). Each heater in the array was individually controlled to keep its temperature at a constant value. The response of the heater and electronic control circuitry was as fast as 15 kHz, much faster than the boiling phenomena being studied. The heater could be operated in full configuration (all 96 heaters were powered) or a reduced set of 3x3 heaters could be powered. An external electric field was imposed over the boiling surface by means of a grid consisting of 4 rods, laid parallel to the surface at a distance of 7 mm from it; voltages up to 10 kV were applied.

2. Experimental Apparatus

A schematic of the experiment is shown in Figures 1 and 2. The experiment package used components from a sounding rocket experiment payload that flew previously on a Terrier-Orion sounding rocket. The primary rack (Figure 1) housed a sealed chamber containing the test fluid at nearly atmospheric pressure, a microheater array to measure the heat transfer distribution during boiling, a rack of electronic feedback circuits, two 30 Hz video cameras, a computer, and a LCD display. All components are contained within a Vertical Equipment Rack (VER) provided by NASA and designed for use on their parabolic aircraft. The secondary rack (Figure 2) contained a high-voltage power supply for the electric field measurements, a transformer to convert from 220 VAC to 110 VAC, a triple output power supply, and a 28 VDC power supply. The components were contained in an Amco 50” Equipment Rack (AER) provided by NASA. A third small rack was used to hold a compressed air bottle.

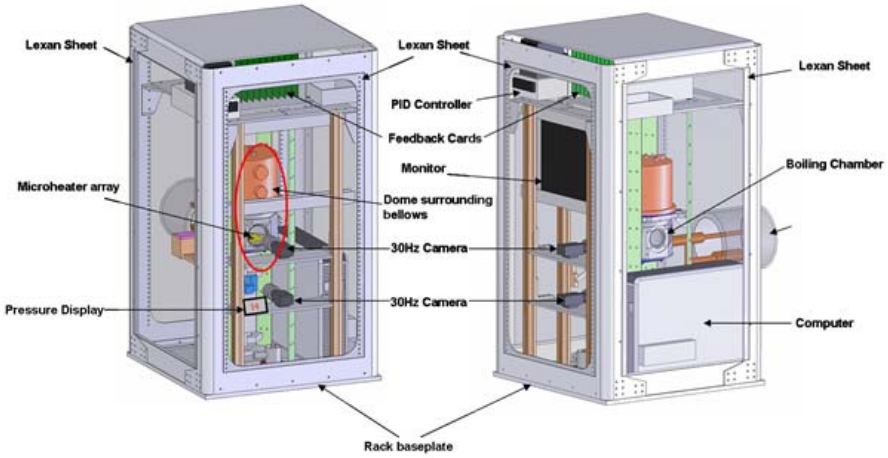

Figure 1. Solid model of the primary rack and its components.

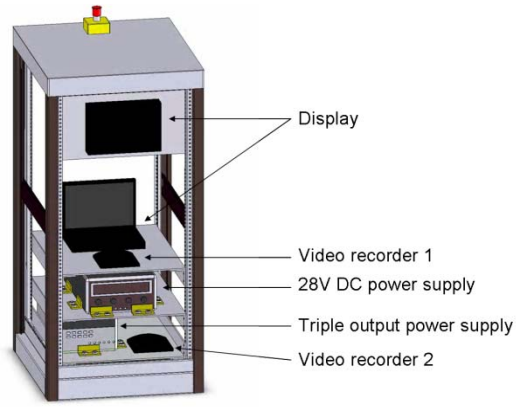

Figure 2. Solid model of secondary rack.

2.1. Description of the subsystems

2.1.1. Test Chamber (primary rack). The test chamber is shown on Figures 3 and 4. The bellows and the surrounding dome allowed the test section pressure to be controlled by varying the air pressure around the bellows. A PID temperature controller, a RTD probe, and Kapton heaters attached to the boiling chamber were used to control the bulk fluid temperature. The chamber was filled with nominally 3 liters of distilled FC-72.

A thorough degassing procedure described in[9] was used to degas the fluid. When degassing the liquid, the test rig was turned upside down. Valves # 1 and #2 were open while valve #3 was closed during the process of filling/emptying the boiling chamber with test liquid (ground procedure). To degas the fluid, valves # 1 and # 2 were open and a vacuum was periodically pulled on the chamber to remove the gas and vapor above the liquid. The final dissolved gas concentration in the liquid was determined using the chamber temperature and pressure, the thermophysical properties of FC-72, and Henry's law. Once completed degassing, Valve # 2 was closed and the rig was brought back in the upright position. Then, valves #1 and #3 were opened momentarily so that the bellows adjusted and the chamber pressure was brought back to 1 atm.

The test chamber included electrodes so electric field effects on boiling could be studied. The cylindrical electrodes (described below) were energized through an insulated conductor fed through a hole drilled into one side of the mating plate between the dome and the lower chamber. The test rig as well as the microheater array was grounded. The electric field was applied when desired between the horizontal microheater array and the electrodes (Figure 5 and Figure 6). The potential difference between the electrode and the heater array could be varied in the range0-10 kVDC.

2.1.2. Microheater Array and Electronic Feedback Circuits (primary rack). A microheater array consisting of 96 platinum resistance heaters deposited in a 10x10 configuration onto a quartz substrate was used to measure the heat transfer distribution during boiling. Each heater in the array was nominally 0.7x0.7 mm^2 in size. Gold power leads 1 μm thick allowed connections to be made to the heaters. Each array element was square with a nominal area of 0.49mm^2. Each heater had a nominal resistance of 200 kΩ and a temperature coefficient of resistance (TCR) of 0.003 K^{-1}. Because the heater lines covered only half of the quartz substrate, images of the bubble could be obtained by looking through the substrate. A photograph of a microheater array is shown on Figure 5.

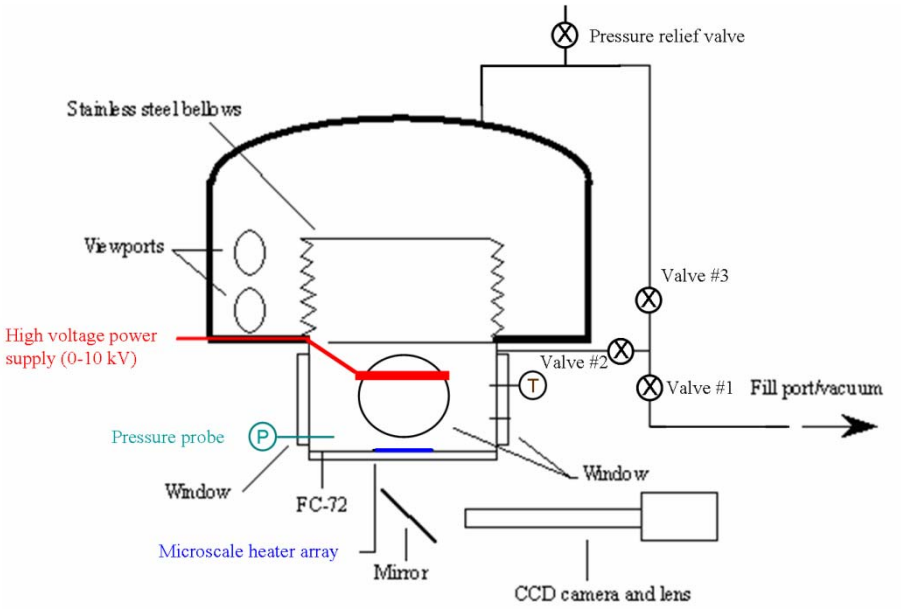

Figure 3. Schematic of the test chamber.

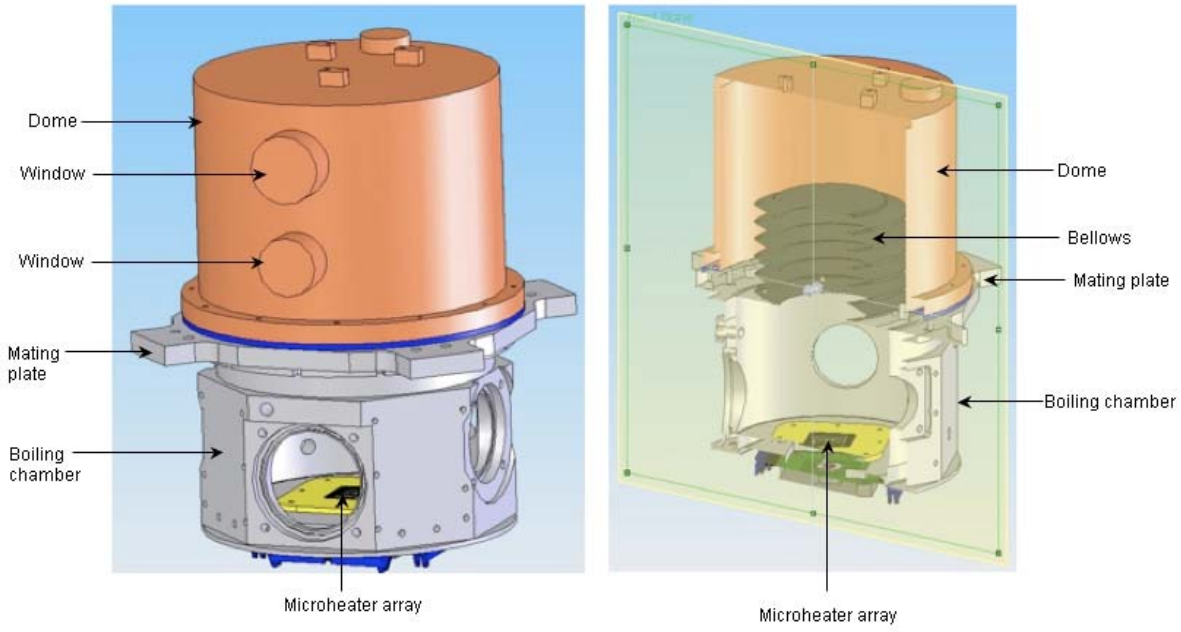

Figure 4. Solid model test chamber.

The power provided to each heater could be individually controlled, therefore it was possible to operate the array in a variety of configurations, and in particular at uniform heat flux or uniform temperature. The constant-temperature mode was chosen for the present series of tests. The temperature of each heater in the array was kept at a specified value by a bank of feedback circuits similar to those used in constant temperature hot-wire anemometry. The reader is referred to Rule and Kim [10] for the details regarding the heater construction and operation. The high feedback frequency (~15 kHz) of the microheater array and a constant temperature boundary condition at the heater surface allowed quasi-steady state data to be obtained during the transition phases of the flight [6].

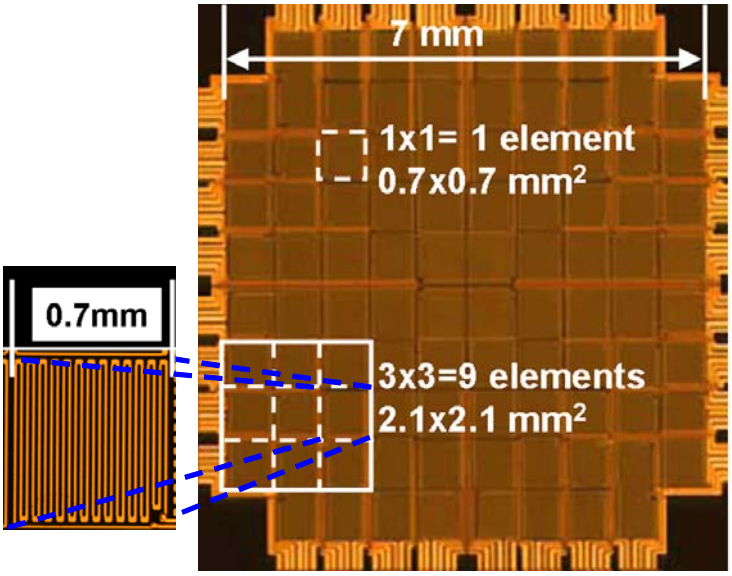

Figure 5. Photograph of microheater array.

2.1.3. High voltage electrode and power supply. The high voltage electrode consisted of a grid of 4 stainless steel rods, 0.9 mm of diameter, 2.1 mm pitch, laid parallel to the heater plane at a distance of 7 mm (from rod axis to heater surface). The grid was fed by a high voltage DC power supply (Brandenburg 590). The high voltage was connected to the rod (positive pole) while the heater acted as ground. The HV power supply was powered at 24 Vdc, and the output high voltage was regulated by an analog input signal 0-10 Vdc. A monitor output indicated the actual value of the high voltage. Figure 6 shows a schematic of the electrode and a plot of the resulting electric field. The maximum field intensity (for an imposed voltage of 10 kV) was 1.2 kV/mm at the surface of electrode rods, which was much lower than the breakdown voltage of 14 kV/mm for FC-72. The average value at the heater surface (in the absence of bubbles) was about 1.22 kV/mm.

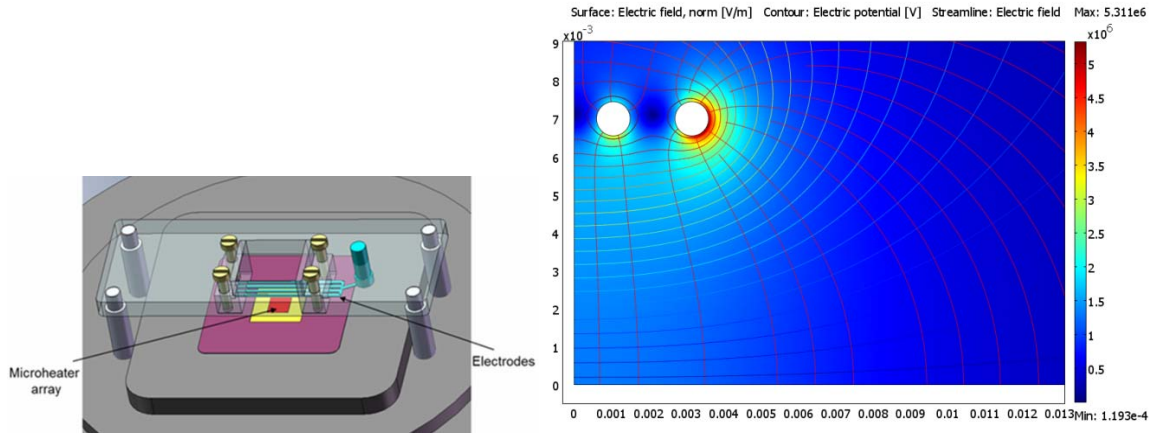

Figure 6. Schematic of the electrode grid and heater (left) and the resulting electrostatic field (right).

2.1.4. Imaging. Two video cameras were used to obtain side and bottom images of the boiling process. One camera used a long focal length lens that imaged the boiling process through the bottom of the heater. The other camera was used to image the bubble life cycle from the side. The frame rate of both cameras was 30 Hz. The output of the video cameras were recorded onto two video recorders housed

in the secondary rack. The video recorder digitized the analog videos and stored them on a USB drive. Two remote controlled DVD players were used as the display for these two cameras.

3. Test Operation

During the present series of test, the apparatus was operated with subcooled fluid conditions (11, 18 and 27 K of subcooling).Due to the thermal dilatation of the fluid, the pressure and hence the saturation temperature increased slightly with decreasing subcooling, as reported in Table 1. The heater temperature was set at an assigned value (from 70 to 95 °C, in steps of 2.5 K) during level flight, and data were acquired through the entire gravitational transient, including macrogravity and transition phases. The heater was used in full configuration (96 heaters) or with a reduced array of 3x3 heater activated; the reduced array was located in between the verticals of two HV electrode rods, i.e. in a zone where the electrical force was directed upwards.

Table 1. Pressure and saturation temperature for the three values of subcooling tested.

Subcooling (K)	Pressure (bar)	Saturation temperature (°C)
27	1.02	57.0
18	1.07	58.5
11	1.12	68.5

An Airbus A300 aircraft flew successive parabolic maneuvers providing ~20 s periods of low-g preceded and followed by ~ 20 s periods of ~1.8g_E. A 1g period lasting a few minutes between successive parabolas was used to set the test parameters. A typical parabola along with the acceleration levels are shown on Figure 7 (left). Thirty parabolas were flown per flight, and three flights were made. The parabolic flight campaign has been primarily used to study phenomena under low-g and hypergravity (>1.5g_E) conditions. However, as can be seen in Figure 7, there was a transition period of approximately 3–5 s when the acceleration varied continuously from hypergravity to low-g and vice versa. This period is generally considered too short for processes to reach equilibrium, and hence unsuitable for making measurements. Nonetheless, data were acquired for this period throughout the transition from hypergravity to low-g and vice versa and was confirmed to be under quasi-steady state conditions as explained below.

The data in Figure7 (right) illustrates the values of gravitational acceleration and heat flux recorded during the pull-up (decreasing gravity) and recovery (increasing gravity) phases along with three steady state experiment results at 1, 1.3, and 1.6 g_E. The data acquired during transition from hypergravity to microgravity (blue gradient symbols) and that from microgravity to hypergravity (red delta symbols) agree, indicating the heat flux depends only on the gravity level and not the direction of change in gravity. Results at steady-state hypergravity conditions (1.3g and 1.6g) along with the reference earth gravity data confirm the quasi-steady boiling during the relatively quick transition period. It was thus possible to obtain quasi-steady boiling data across a continuous range of gravity levels between ~0 to 1.8 g_E.

The electric field was activated before the beginning of a parabola (to assess its effect in variable gravity) or during the micro-g phase, to investigate the flow pattern and heat transfer changes due to its application in reduced gravity.

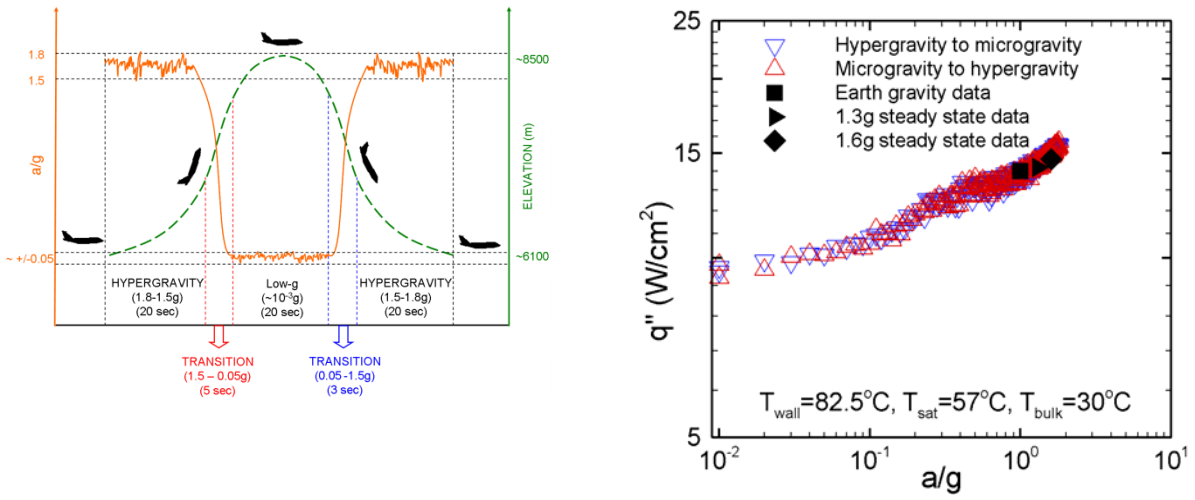

Figure 7. Gravitational transient during parabolic flight in A300 "Zero-G and boiling data (heat flux) during gravitational transient.

4. Results and Discussion

4.1. Large heater- 7x7 mm^2

4.1.1. High subcooling data. Figures 8-9 show the effect of the application of electric field during the gravitational transient: heat flux data are reported versus gravity acceleration, with and without electric field. The figures show clearly that the electric field is ineffective above a threshold value of gravity acceleration. While it improves the boiling performance below a value of gravity acceleration of 0.1-0.2 g_E, at least for moderate wall superheat (Figure 8), this effect vanishes at a larger wall superheat (Figure 9). The boiling process is dominated by buoyancy for sufficiently high values of gravity acceleration [6], while it is dominated by surface tension at lower values of g; these two regimes are characterized by a different boiling flow pattern; in the gravity-dominated regime several individual bubble are present and detaching over the heater, while in the surface-tension dominated regime a single coalesced bubble whose size is of the order of the heated surfaces forms over it.

Boiling curves in microgravity are shown in Figure 10. Here, the low-g data (with and without electric field) are compared with the boiling curve in normal gravity, where the application of electric field has little effect. Images of the boiling flow patterns, as observed from the bottom of the semi-transparent heater, are also shown in correspondence with the related data points. It can be noted that the boiling performance in microgravity is worse than in normal gravity whether or not an electric field is applied; however the application of electric field in low-g improves the heat flux of about 13% at intermediate wall superheats, while its effect is lower or negligible at higher and lower wall superheat. The maximum improvement can be associated to a change in flow pattern: the single coalesced bubble residing over the heater is split in smaller ones by the electrical forces.

From the analysis of these data, it may be concluded that the application of electric field, at least in the present geometrical configuration, is effective only in the surface-tension-dominated region, and its effect is strongly reduced or vanishes at all at high values of wall superheat. This last effect may be due to the increased bubble size; when the bubble is larger, electrical forces may be too weak to break up the large coalesced bubble that forms on the heater.

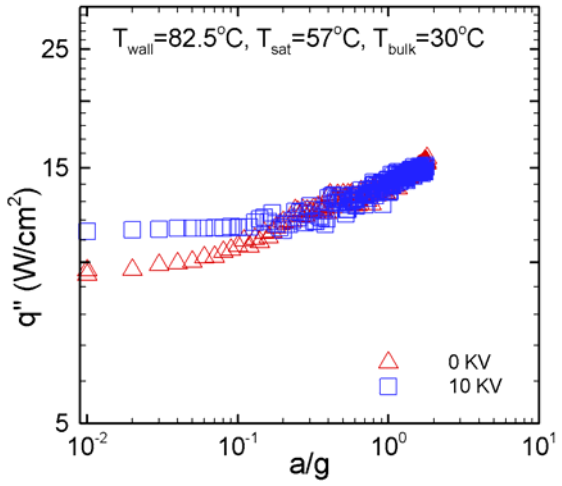

Figure 8. Values of heat flux vs. gravitational acceleration, at intermediate wall superheat and high subcooling.

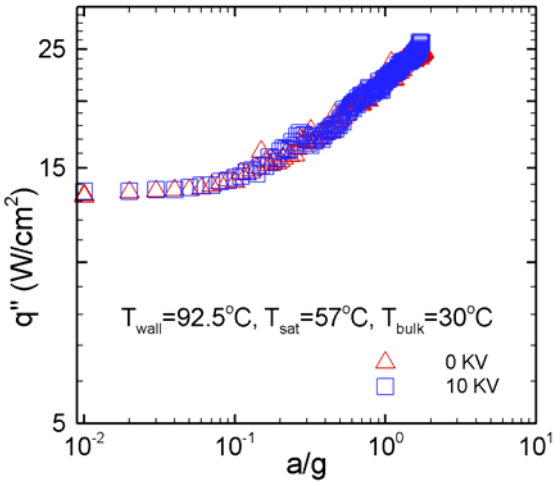

Figure 9. Values of heat flux vs. gravitational acceleration, at high wall superheat and high subcooling.

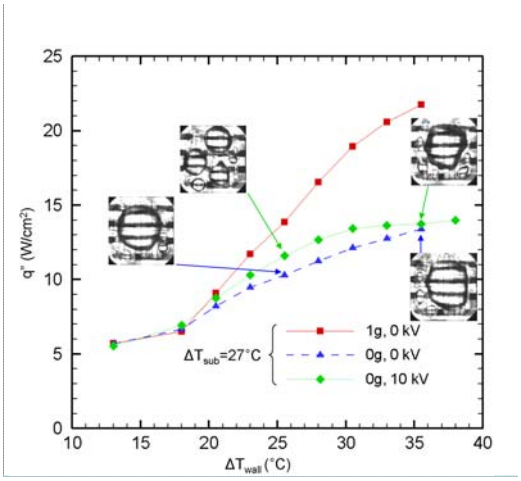

Figure 10. Boiling curves in normal and reduced gravity, high subcooling, full heater.

4.1.2. Intermediate and small subcooling data. Figure 11-13and 14-16 report the same data as in former section for the intermediate (18 K) and small (11 K) subcooling, respectively. Similar qualitative observations as in former section may be made. In particular it may be noted that an improvement due to the application of EF takes place also at high wall superheat. By comparing Figs. 8, 11 and 14, it may be noted that in presence of EF a plateau is attained when gravity drops below about 0.1 g_E. Below 0.1g_E, boiling is surface tension dominated and the effect of gravity acceleration is very small [6]. As a result, the heat transfer is unaffected, however, is larger compared to the case without electric field. In effect, it can be concluded that under low-g conditions, the "equivalent gravity field" due to the applied electric field (10 kV, 7 mm) at intermediate superheats is approximately 0.1 g_E. Furthermore, the improvement due to EF application is more marked with decreasing subcooling, and for intermediate subcooling at low wall superheat the same boiling performance as in normal gravity is restored.

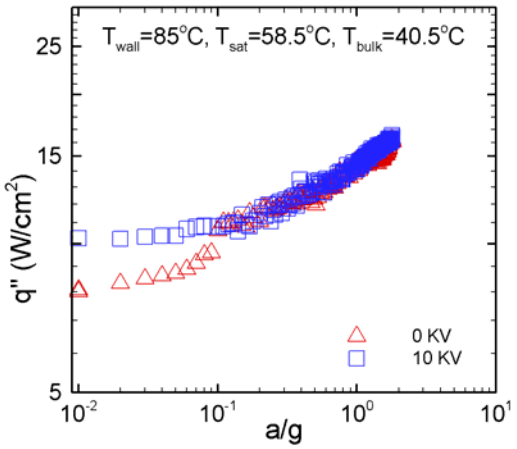

Figure 11. Values of heat flux vs. gravitational acceleration, at intermediate wall superheat and intermediate subcooling.

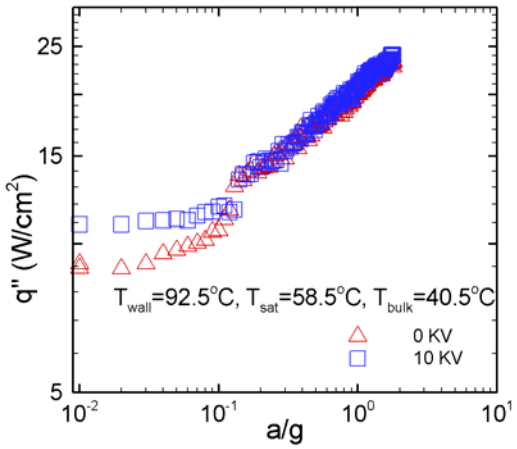

Figure 12. Values of heat flux vs. gravitational acceleration, at high wall superheat and intermediate subcooling.

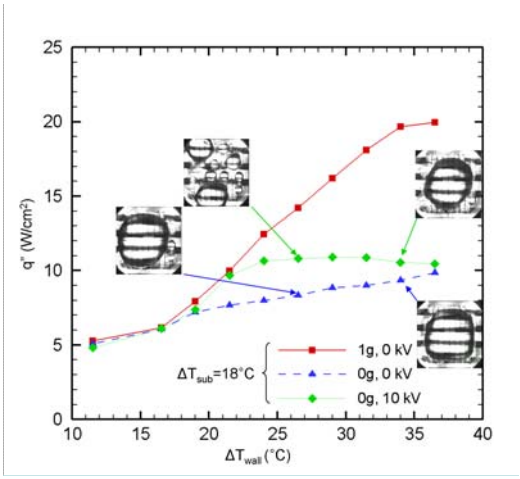

Figure 13. Boiling curves in normal and reduced gravity, intermediate subcooling, full heater.

4.2 Small heater- 2.1x2.1 mm²

The boiling curves for the small heater (3x3) configuration are shown on Figures 17-19. At high subcooling the application of electric field restores the same heat transfer performance as in normal gravity for the lower wall superheats: the electric field becomes less effective at higher wall superheats. The heat transfer degradation in microgravity is less marked in this case. For intermediate subcooling the enhancement takes place mostly at intermediate wall superheat. Finally, at low subcooling, the application of electric field is less effective. Generally, on the small heater, the bubble does not split into smaller ones under the action of electric field, but its size is reduced due to the contribution of electrical overpressure in the surrounding liquid. The observation of videos shows that convective patterns around the bubble are noticeably enhanced when the electric field is applied: this is likely due to electroconvection.

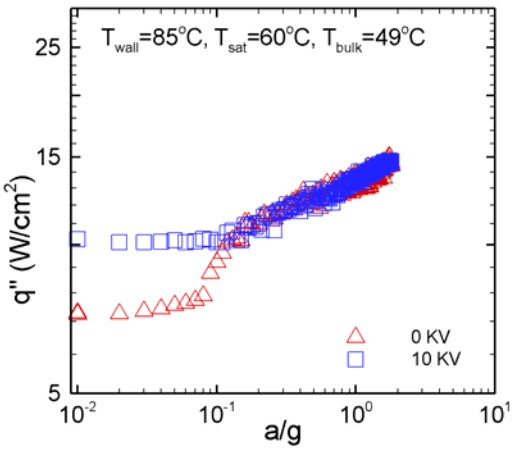

Figure 14. Values of heat flux vs. gravitational acceleration, at intermediate wall superheat and low subcooling.

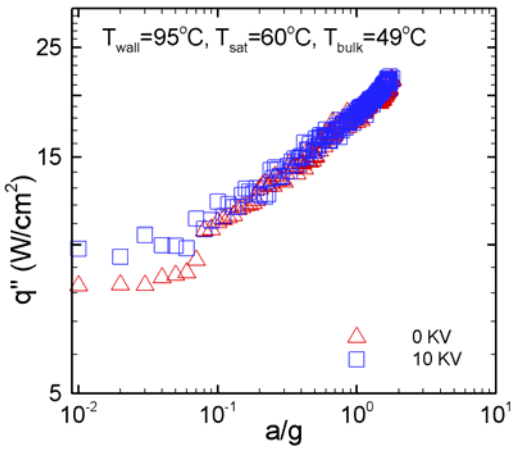

Figure 15. Values of heat flux vs. gravitational acceleration, at high wall superheat and low subcooling.

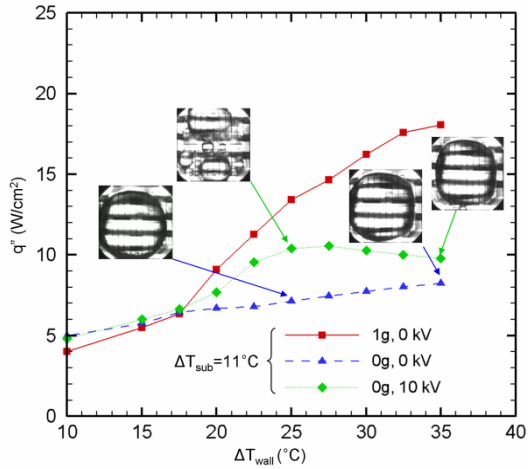

Figure 16. Boiling curves in normal and reduced gravity, low subcooling, full heater.

4.3 Resume of heat transfer improvement

Table 2 summarizes the heat transfer improvements generated by the application of electric field in low-g in different conditions. It can be noted that the increase in performance is more marked for the small heater at intermediate wall superheat.

Table 2. Summary of heat transfer enhancements.

	7x7 mm² heater		2.1x2.1 mm² heater	
SUBCOOLING	Increase at intermediate superheat	Increase at high superheat	Increase at intermediate superheat	Increase at high superheat
HIGH	13 %	1 – 5 %	15 %	3 – 7 %
MEDIUM	33 %	5 – 10 %	55 %	20 – 30 %
LOW	46 %	15 – 20 %	35 %	20 – 30 %

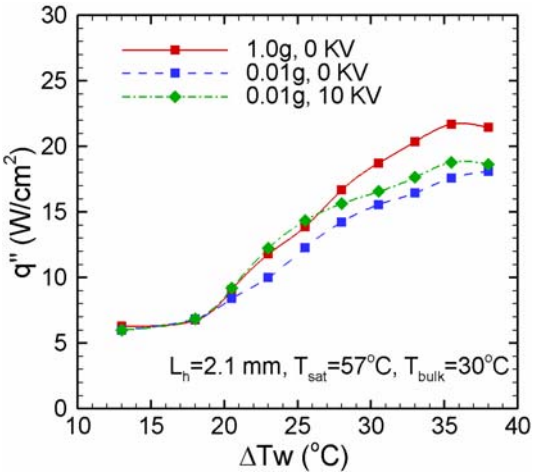

Figure 17. Boiling curves in normal and reduced gravity, high subcooling, 3x3 heater.

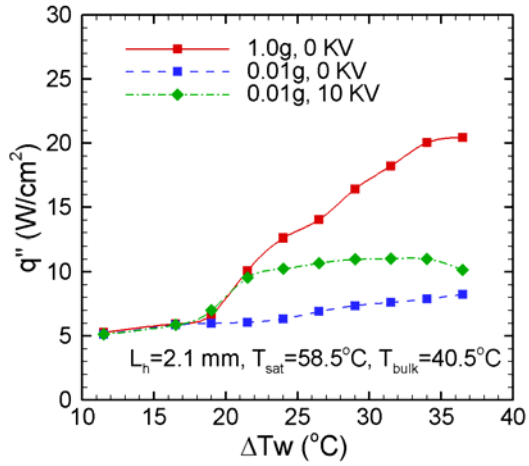

Figure 18. Boiling curves in normal and reduced gravity, intermediate subcooling, 3x3 heater.

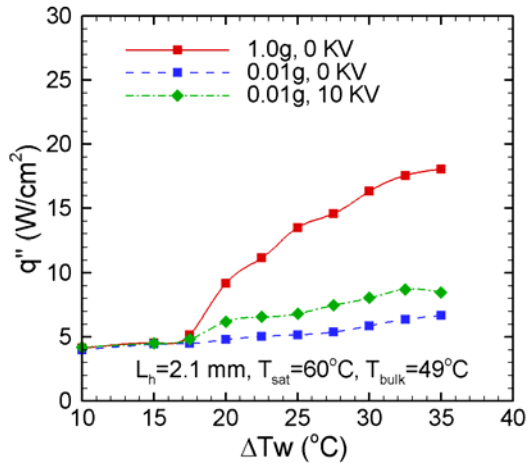

Figure 19. Boiling curves in normal and reduced gravity, low subcooling, 3x3 heater.

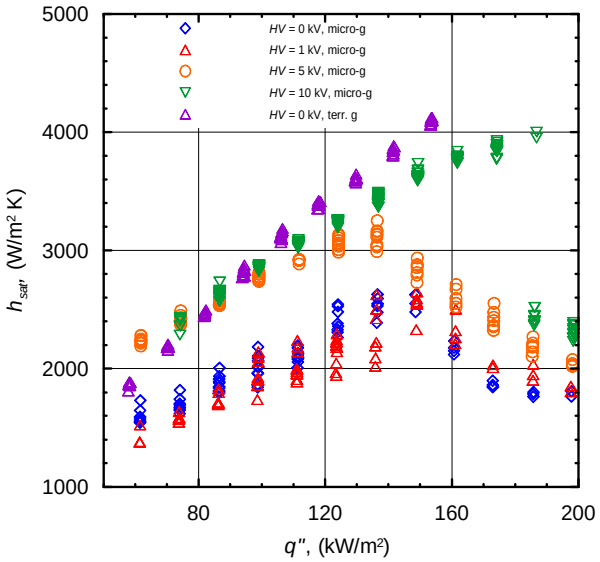

Figure 20. Heat transfer coefficient h_{sat} in normal and reduced gravity in ARIEL apparatus, for a subcooling of 16.6 K, from [8].

4.4. Comparison with former results (ARIEL apparatus)

The ARIEL apparatus [8], operated in orbital flight (gravity acceleration lower than 10^{-4} g_E) during Foton-M2 mission, consisted mainly in an aluminum vessel of about 1 liter volume, containing the test fluid, FC-72. The active heating element consisted of a square uniform layer of 20x20 mm, with a 40-nm thick gold layer deposited via sputtering over a 10-mm-thick ZnS substrate, and was operated at constant power, achieving heat fluxes up to 200 kW/m^2. The pressure was kept constant at 100±3 kPa, with subcooling ranging from 6.6 to 16.6 K. An external electrostatic field with a voltage up to 10 kV dc was imposed by means of a grid of five parallel stainless steel rods, 1 mm in diameter, spaced 5 mm and laid parallel to heater, at a distance 5 mm above it (from rod axis to plate).

Data in microgravity, with no electric field applied, exhibited a degradation of boiling performance: the heat transfer coefficient showed to be closely linked to the boiling pattern, and in particular to the presence and evolution of the big mass of vapor over the heater, originated by bubble coalescence. The heat transfer degradation was reduced or even cancelled with the application of the electrostatic field, that, especially for high applied voltages, contrasted the formation of the large vapor mass, improved the bubble removal from the heated surface and restored a performance more similar to terrestrial one. This improvement, however, was no more effective for increasing heat flux, even for the highest value of the voltage applied during the tests. An example is shown in Fig.20. Although the heater morphology and its mode of operation were different, it may be concluded that there is a good qualitative agreement between the results of the two tests.

5 Conclusions

Results of variable gravity pool boiling with FC-72 have been reported in this paper; in particular, the effects of an external electric field on the bubble dynamics and associated heat transfer. The main experimental results can be summarized as follows.

- Boiling heat transfer is generally degraded in low-g; the degradation is discontinuous when transition from buoyancy dominated to surface-tension-dominated boiling occurs. This discontinuity is associated to a transition in flow patterns (from multiple departing bubbles to a large coalesced non-departing bubble covering the entire heater).
- The effect of electric field is most pronounced at lowest subcooling.

- The effect of electric field at a given subcooling is more pronounced at intermediate wall superheats.
- The baseline heat transfer (0 kV) is already high at higher subcoolings (higher condensation / increased thermocapillary convection) resulting in smaller percentage increase with electric field.
- Both increased subcooling and electric field inhibit bubble coalescence. At higher wall superheats, coalescence is less inhibited by application of the electric field.
- Lower subcooling results in larger coalesced bubbles.
- The coalesced bubble is split by the application of EF into smaller bubbles which slide to the side at lower subcoolings. The coalesced bubble is split into smaller bubbles which reside on the heater (with increased condensation at the bubble top) at larger subcoolings.
- Small (2.1 mm) and large (7 mm) heaters show similar trends; the relative increase in heat transfer is generally higher for the small heater.

In summary, the electric field is effective in reducing the size of the detaching bubbles, and increasing the heat transfer compared to the values in low-g, although its effectiveness decays as the heat flux/superheat increases. From the analysis of flow patterns, it may be concluded that contrasting bubble coalescence leads to an enhancement of boiling in reduced gravity.

The present results compare well with former ones obtained in the ARIEL apparatus [8] operated in orbital flight, and extend the explored range of parameters in terms of heater size, subcooling, gravity and electric field intensity. Further analysis is ongoing to better explain the physical mechanisms governing the boiling phenomena in the presence of electric field or less.

Acknowledgements
The authors would like to thank the European Space Agency for accommodating the experiment on the 52ndESA Parabolic Flight Campaign organized May 2010, and Novespace for the assistance given in setting up the apparatus on board of the aircraft.

References

[1] Siegel R Keshock E G, Effects of reduced gravity on nucleate boiling bubble dynamics in saturated water, *AICHE Journal*, **10**,4, 1964, 509.
[2] Di Marco P, Kim J, Ohta H, Boiling Heat Transfer in Reduced Gravity Environments, *Adv. in Multiphase Flow and Heat Transfer*, L. Cheng and D Mewes Eds,. Bentham Publishing Co. **1**, Ch.2, 2009, 53.
[3] Di Marco P, Influence of force fields and flow patterns on boiling heat transfer performance, keynote lecture, *Proc. of the International Heat Transfer Conference, IHTC14, August 8-13, 2010*, Washington, DC, USA, (CD-ROM), paper IHTC14-23409, 1-18.
[4] Straub J, Boiling Heat Transfer and Bubble Dynamics in Microgravity, *Adv. Heat Transfer*, **35**, 2001, 57.
[5] Merte H, Some parameter boundary governing microgravity pool boiling modes, *Ann. N.Y. Acad. Sci.*, **1077**, 2006, 629-649.
[6] Raj R, Kim J, and McQuillen J,Subcooled Pool Boiling in Variable Gravity Environments, *ASME Journal of Heat Transfer*, **131**, 2009, 091502-1.
[7] Di Marco P, Grassi W, Pool boiling in microgravity: old and recent results, *Multiph. Sci. and Technology*, **19**, 2, 2007, 141.
[8] Di Marco P, Grassi W, Effects of external electric field on pool boiling: comparison of terrestrial and microgravity data in the ARIEL experiment, *Experimental Thermal and Fluid Science*, **35**,5, 2011, 780.
[9] Henry C D, Kim J, and McQuillen J, Dissolved Gas Effects onThermocapillary Convection During Subcooled Boiling in Reduced GravityEnvironments, *Int. J. Heat Mass Transfer*, 2006, **42**, 919.
[10] Rule T D, and Kim J, Heat Transfer Behavior on Small HeatersDuring Pool Boiling of FC-72, *ASME J. Heat Transfer*, **121**(2), 1999, 386.